applied sciences

MDPI

Article

The Diatom *Cylindrotheca closterium* and the Chlorophyll Breakdown Product Pheophorbide *a* for Photodynamic Therapy Applications

Assunta Saide †, Gennaro Riccio †, Adrianna Ianora and Chiara Lauritano *

Ecosustainable Marine Biotechnology Department, Stazione Zoologica Anton Dohrn, 80121 Naples, Italy
* Correspondence: chiara.lauritano@szn.it; Tel.: +39-081-5833221
† These authors contributed equally to the work.

Abstract: Microalgae, eukaryotic unicellular plants that are distributed worldwide, have been shown to exert anti-proliferative and anticancer activities on various human cancer cell lines. An example of a microalgal bioactive compound is a chlorophyll breakdown product named Pheophorbide *a* (Pp*a*), which has been reported to have anti-proliferative properties against various cell lines. This compound has also been tested with light exposure in photodynamic therapy for cancer treatment. In this paper, we screened eleven marine microalgae against a panel of cancer cells, and evaluated the synergistic anti-proliferative effect with Pheophorbide *a*, with and without photo-activation. The results showed significant anti-proliferative activity against melanoma cells when Pp*a* was combined with fraction E of the diatom *Cylindrotheca closterium* plus 1 h photo-activation. Its activity was also analyzed using gene expression and Western blot experiments. Altogether, these data give new insights into the possible application of microalgae for photodynamic therapy.

Keywords: microalgae; *Cylindrotheca closterium*; Pheophorbide *a*; photodynamic therapy; cancer; biotechnological applications

check for updates

Citation: Saide, A.; Riccio, G.; Ianora, A.; Lauritano, C. The Diatom *Cylindrotheca closterium* and the Chlorophyll Breakdown Product Pheophorbide *a* for Photodynamic Therapy Applications. *Appl. Sci.* **2023**, *13*, 2590. https://doi.org/10.3390/app13042590

Academic Editor: Leonel Pereira

Received: 9 January 2023
Revised: 9 February 2023
Accepted: 13 February 2023
Published: 17 February 2023

1. Introduction

Cancer ranks as one of the leading causes of death worldwide (https://www.who.int/health-topics/cancer#tab=tab_1; accessed on 19 January 2023). Photodynamic therapy (PDT) is an evolving strategy for the non-invasive treatment of superficial tumors and is used for both pre-malignant and various cancerous diseases [1]. It consists of the administration of a photosensitiser drug (or pro-drug) successively and locally exposed to visible light with minimal risk of toxicity [1,2]. A chlorophyll derivative product, named Pheophorbide *a* (Pp*a*), is a photosensitizer that can have anticancer properties [3]. Interestingly, Pp*a* showed anticancer properties with or without PDT and with or without conjugation with other chemotherapeutic drugs [3]. In particular, Pp*a* showed anti-proliferative activities on hepatocellular carcinoma (Hep3B; [4]), uterine sarcoma (MES-SA; [5]), breast adenocarcinoma (MDA-MB-231, MCF-7; [6,7]), oral squamous cell carcinoma (YD10B; [8]) and glioblastoma cells (U87MG; [9]). The mechanism of action is not always reported, and, when studied, it showed a cell-death generally induced by intrinsic or extrinsic apoptosis [3].

Microalgae are characterized by enormous biodiversity in terms of species adapted to living in very different environments, in both marine and freshwater ecosystems, including extreme conditions. Their culturing is faster compared to macroorganisms and they are known to produce a plethora of molecules with possible exploitation in different industrial fields [10,11]. Most common bioactive molecules from microalgae belong to pigments, polyphenols, polysaccharides, lipids, oxylipins, glycolipids, steroids, peptides and macrolides (as reviewed by [12]). These molecules have demonstrated different activities, such as anticancer, anti-diabetes, anti-atherosclerosis, antiviral, antibacterial and

immunomodulatory activities [13–21], and have also found applications in the aquaculture (such as for fish oil replacement in fish diets, as live prey diets or powder products), biodiesel and biomaterial sectors [22–26]. Considering that some microalgae (biomass or extracts) have received the "GRAS" (generally recognized as safe) status [27], there are now various microalgae-derived powder-based products on the market and recent investigations have also proposed them as ingredients in fresh pasta, cookies and yogurt [28–30].

In this study, various microalgal species (i.e., two *Chlamydomonas* sp., *Dunaliella tertiolecta*-Chlorophyta, *Asterionellopsis glacialis*, *Cylindrotheca closterium*, *Ditylum brightwellii*, *Trieres mobiliensis*, *Pseudo-nitzschia arenysensis*, *Pseudo-nitzschia fraudulenta*-Bacillariophyta, *Scrippsiella acuminata*-Miozoa, *Rhinomonas reticulata*-Cryptista) were tested on human cancer cell lines (i.e., melanoma, hepatocarcinoma and myeloma) and a non-cancerous cell line. The microalgae selected for this study included both diatoms, flagellates and one dinoflagellate, in order to screen different microalgal classes and increase the probability of finding activity. In addition, considering that different strains of the same genus may exert different bioactivities [10], we also selected two *Chlamydomonas* (Chlorophyta) and two *Pseudo-nitzschia* species (Bacillariophyta). Some of these microalgae were already tested in other studies for other possible applications. For example, Lauritano et al. [31] showed that the diatom *Cylindrotheca closterium* had anti-inflammatory activity and identified lysophosphatidylcholines and chlorophyll-derived molecules as active components. Total extracts of the diatom *Trieres mobiliensis* (formerly *Odontella mobiliensis*) also showed anti-inflammatory activity on THP-1 (human acute monocytic leukemia cell line) with dose-dependent inhibition of tumor necrosis factor-α production [10]. Pasquet et al. [32] demonstrated a strong anti-proliferative activity of the flagellate *Dunaliella tertiolecta* (Chlorophyta) on the breast cancer cell line MCF-7 and the prostate cancer cell line LNCaP. The natural xanthophyll pigment violaxanthin was identified as the bioactive component of the active *D. tertiolecta* dichloromethane extracts [32]. Recently, Martinez and co-workers [16] tested another *Dunaliella tertiolecta* strain (CCMP 1320) on melanoma, hepatocellular liver carcinoma and two lung adenocarcinoma cell lines (A2058, HepG2, HCC827 and Calu-3, respectively) and isolated a glycerol 1-(9Z,12Z,15Z-octadecatrienoate)-2-(4Z,7Z,10Z,13Z-hexadecatetraenoate)-3-O-b-D-galactopyranoside as the active component with anti-proliferative activity against melanoma. The focus of this research was to investigate the effects of microalgal extracts on various cancer cell lines (including both circulating and solid tumor cell lines) combined with the pure compound Pheophorbide *a*, with and without light exposure, to evaluate their possible application for PDT in cancer treatment.

2. Materials and Methods

2.1. Microalgae Culture

A series of microalgae (Table 1), including both diatoms, flagellates and one dinoflagellate, were cultivated in triplicate in 10L polycarbonate bottles. *Cylindrotheca closterium*, *Ditylum brightwellii*, *Trieres mobiliensis*, *Pseudo-nitzchia arenysensis*, *Pseudo-nitzchia fraudulenta* and *Scrippsiella acuminata* belong to the Stazione Zoologica Anton Dohrn culture collection. They were previously collected in the Mediterranean Sea and identified using microscopy. The other microalgae were bought at the Roscoff culture collection (RCC), the Provasoli–Guillard National center for marine algae and microbiota (originally named culture collection of marine phytoplankton, from which the abbreviation code CCMP), and culture collection of algae and protozoa (CCAP). Diatoms were grown in Guillard's f/2 medium [33], flagellates in f/2 without silicates and the dinoflagellate in Keller medium [34]. The triplicates were cultured at 19 °C with a 12:12 h light:dark cycle and at 100 µmol photons m^{-2} s^{-1} in a dedicated controlled chamber (as in [10]). An inoculum of 5000 cells·mL^{-1} was used and algae were centrifuged (for 30 min at 4 °C at 3900× *g*) at the end of the stationary phase (selected because this is the stage when secondary compounds may be produced in higher quantities; [35]). Culture growth was evaluated from samples fixed with one drop of Lugol (about 2% final concentration) and counted in a Sedgewick Rafter counting chamber under

an Axioskop 2 microscope (20×) (Carl Zeiss GmbH, Jena, Germany). Samples were stored at −80 °C until successive chemical analysis.

Table 1. The table reports the microalgal species cultured for this study, name abbreviation (Abb), their class, growth media, sampling location and cell concentration at the end of the stationary phase when they were pelleted and stored for the successive analyses.

Species	Abb	Class	Growth Media	Sampling Location	Concentration at the End of the Stationary Phase
Asterionellopsis glacialis (RCC1712)	*Ag*	Fragilariophyceae	F/2	English Channel	10^5
Chlamydomonas sp. (CCMP2536)	*CspA*	Chlorophyceae	F/2-Si	Mediterranean Sea (Almeria harbor)	10^6
Chlamydomonas sp. (CCMP225)	*CspB*	Chlorophyceae	F/2-Si	Nantucket Sound	10^6
Cylindrotheca closterium	*Cc*	Bacillariophyceae	F/2	Mediterranean Sea (Adriatic Sea)	4×10^5
Dunaliella tertiolecta (CCMP1320)	*Dt*	Chlorophyceae	F/2-Si	Unknown	2×10^6
Ditylum brightwellii	*Db*	Mediophyceae	F/2	Mediterranean Sea	10^5
Trieres mobiliensis	*Om*	Coscinodiscophyceae	F/2	Mediterranean Sea	10^5
Pseudo-nitzchia arenysensis	*Pa*	Bacillariophyceae	F/2	Mediterranean Sea	3×10^5
Pseudo-nitzchia fraudulenta	*Pf*	Bacillariophyceae	F/2	Mediterranean Sea	3×10^5
Rhinomonas reticulata (CCAP 995/2)	*Rr*	Cryptophyceae	F/2	Mediterranean Sea	10^5
Scrippsiellaacuminata	*St*	Dinophyceae	K	Mediterranean Sea	10^4

2.2. Chemical Extraction

Extractions were performed according to Martinez et al. [16]. For the microalga, *Cylindrotheca closterium*, an additional step of fractionation was done according to Cutignano et al. [36].

2.3. Cells

DMEM medium was used for human melanoma cells (A2058; ATCC® CRL-11147™) and human keratinocytes (HACAT; CLS n. 300493; https://www.ceinge.unina.it/en/cell-cultures, accessed on 17 January 2022; CEINGE, Napoli, Italy), EMEM for hepatocellular liver carcinoma cells (HepG2; ATCC® HB-8065™). Media were supplemented with 10% fetal bovine serum, 50 U·mL^{-1} penicillin, and 50 µg·mL^{-1} streptomycin (Sigma–Aldrich, St. Louis, MO, USA). Human plasma cell myeloma (JJN3; DSMZ n. ACC541; https://www.ceinge.unina.it/en/cell-cultures, accessed on 17 January 2022; CEINGE, Napoli, Italy) were cultured in DMEM HG + ISCOVE (1:1), 20% fetal bovine serum and 2% glutamine.

2.4. Antibody

Antibodies (from Cell Signaling Technology; Danvers, MA, USA) used were: rabbit monoclonal anti-glutathione peroxidase 4 (GPX4; 52455s), rabbit monoclonal anti-tubulin (9F3, 2118s), rabbit monoclonal anti-nuclear receptor coactivator 4 (NCOA4; E8H8Z, 66849s), rabbit monoclonal anti-glyceraldehyde 3-phosphate dehydrogenase (GAPDH; 14C10, 2118s), the rabbit monoclonal anti-B-cell lymphoma (Bcl-2, D17C4, 3498S), rabbit monoclonal anti-Bcl-2-associated X protein (Bax, D2E11, 5023S), anti-rabbit IgG, HRP-linked antibody (7074s) and anti-mouse IgG, and HRP-linked antibody (7074s).

2.5. In Vitro Cell Viability

To study the effects of microalgal extracts and Pheophorbide *a* (CAS15664-29-6; Santa Cruz Biotechnology, Inc., Dallas, TX, USA) on cell viability, A2058, HepG2 and HACAT cell lines were seeded in 96-well microtiter plates (1×10^4 cells·well^{-1}) and incubated at 37 °C for 24 h. Then, fresh medium was used, including extracts and Pp*a*: (1) 50 µg·mL^{-1}

microalgal extract + 10 μg·mL^{-1} Pp*a*, (2) 25 μg·mL^{-1} microalgal extract + 10 μg·mL^{-1} Pp*a*, (3) 25 μg·mL^{-1} microalgal extract + 5 μg·mL^{-1} Pp*a*, (4) 10 μg·mL^{-1} Pp*a*. Extracts were dissolved in dimethyl sulfoxide (DMSO; maximum concentration 1% *v*/*v*) and tested at least in triplicate. After 72 h of incubation, cell viability was evaluated using the MTT assay (3-(4,5-dimethyl-2-thizolyl)-2,5-diphenyl-2H-tetrazolium bromide; A2231,0001, Applichem Panreac Tischkalender, Darmstadt, GmbH) as in [37]. For JJN3 cells, grown mostly as single cells in suspension, after 72 h of incubation, cell viability was assessed using Orangu™ Cell Counting Solution (OR01-1000) by directly adding it to the medium. After 1 h in the incubator, the absorbance was measured at 450 nm in the same above-mentioned microplate reader. Photo-activation experiments were performed by exposing cells treated with extracts, fractions and/or Pp*a* for 1 h under 1.000 Lux·m^{-2}, immediately followed by the MTT or Orangu assay.

The viability of the melanoma cell line A2058 exposed to Pp*a* (i.e., 0.005, 0.01, 0.05, 0.1, 0.5, 1.0, 5.0, 10 and 50 μM) and photo-activation for 1 h (to evaluate the combination of Pp*a* and light for possible photodynamic therapy) was also evaluated with the MTT protocol. *Cylindrotheca closterium* (Cc) was the most active species combined with Pp*a* and further fractionation and fraction/Pp*a* testing was performed (for 24 h). When photo-activation was tested, 1 h light exposure was performed before the MTT assay (as above). Cell survival was expressed as a percentage of viable cells in treated samples, with respect to untreated control cultures with only DMSO.

2.6. RNA Extraction, Retrotranscription and PCR Array

RNA was extracted from A2058 cells seeded in 6-well plates (at 500,000 cells/well) for 16 h and then incubated with either Pp*a* 1.91 μM or Cc fraction E 10 μg·mL^{-1}, or with a combination of Pp*a* 1.91 μM and Cc fraction E 10 μg·mL^{-1}, for 14 h at 37° C followed by 1 h of photo-activation. RNA was extracted following Trisure Reagent (Meridian Bioscience, Memphis, TN, USA) manufacturer's instructions. RNA quality, quantity and purity check, retrotranscription and PCR array (cat. PAHS-212ZE-4, Qiagen, Hilden, Germany) were performed as in Riccio et al. [37]. The results described the changes in gene expression between cells treated in the presence of Pp*a* 1.91 μM, Cc fraction E 10 μg·mL^{-1}, or a combination of Pp*a* 1.91 μM plus Cc fraction E 10 μg·mL^{-1}, each one plus photo-activation, and cells treated in the presence of DMSO alone. Only expression values greater than a two-fold difference with respect to the controls were considered significant.

2.7. Protein Extraction and Western Blotting

A2058 cells seeded for protein extraction were incubated with either Pp*a* 1.91 μM, Cc fraction E 10 μg·mL^{-1}, or a combination of Pp*a* 1.91 μM and Cc fraction E 10 μg·mL^{-1} for 14 h, followed by 1 h photo-activation. Protein extraction and Western blot were performed as in Riccio et al. [37]. GAPDH was used as reference to normalize immunoreactive bands. Arithmetic means ± the standard deviations (SD) were calculated and compared using a two-tailed Student *t* test. Differences at $p < 0.05$ were considered significant.

3. Results

3.1. Anti-Proliferative Activity of Microalgal Extracts

Total extracts of *Asterionellopsis glacialis*, *Chlamydomonas* sp. (CCMP2536), *Chlamydomonas* sp. (CCMP225), *Cylindrotheca closterium*, *Dunaliella tertiolecta*, *Ditylum brightwellii*, *Trieres mobiliensis*, *Rhinomonas reticulata*, *Pseudo-nitzschia arenysensis*, *Pseudo-nitzschia fraudolenta* and *Scrippsiella acuminata* in combination with Pheophorbide *a* were screened on various cancer cells. The results showed that the most active combination was *Cylindrotheca closterium* and Pheophorbide *a* against A2058 melanoma cell lines (Supplementary Table S1). A2058 cells were incubated in the presence of (1) 50 μg·mL^{-1} microalgae extract + 10 μg·mL^{-1} Pp*a*, (2) 25 μg·mL^{-1} microalgae extract + 10 μg·mL^{-1} Pp*a*, (3) 25 μg·mL^{-1} microalgae extract + 5 μg·mL^{-1} Pp*a*, (4) 10 μg·mL^{-1} Pp*a*. As shown in Supplementary Table S1, the

first combination showed 32% cell viability while the second and the third showed 46% cell viability after incubation.

3.2. Pheophorbide a Activity against Melanoma Cells

Pp*a* was evaluated at concentrations from 0.001 to 20 µM in order to establish IC_{50} values, (Figure 1a) for 24 h followed by 1 h photo-activation. IC_{50} value of Pp*a* on A2058 cells was 1.91 µM. Then Pp*a* (at IC_{50} concentration) was tested in combination with fractions (from A to E) of Cc at 25 µg·mL^{-1} (plus 1 h light exposure) in order to evaluate possible combinatorial antiproliferative effects (Figure 1b). Fraction E was the most active in reducing cell viability below 20% (i.e., 14%). At this point, A2058 cells were treated for 24 h in the presence of fraction E alone followed by 1 h photo-activation and fraction E in combination with Pp*a* followed by 1 h photo-activation at different concentrations (Figure 1c) to evaluate the IC_{50} of fraction E. IC_{50} of fraction E in the absence or in the presence of Pp*a* was very similar (10.17 ± 0.20 and 9.9 ± 0.17 µg·mL^{-1}, respectively). On the contrary, lower activity was observed against normal human keratinocytes (HaCat, Figure S1).

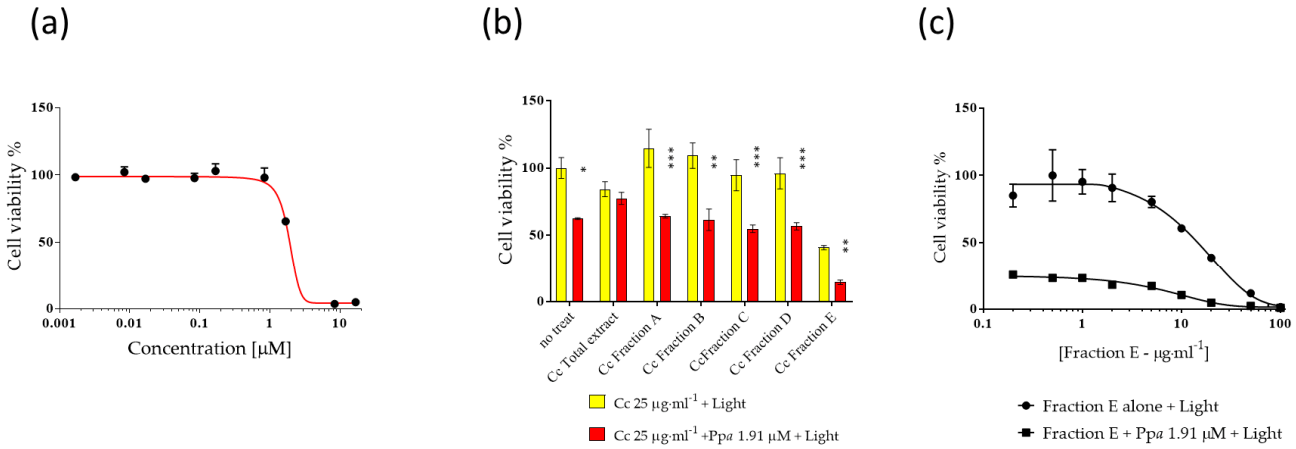

Figure 1. Activity of Pheophorbide *a* (Pp*a*) and *Cylindrotheca closterium* (Cc) against melanoma cells (A2058). The figure shows (**a**) the dose-dependent activity of Pp*a*, (**b**) Cc fractions (from A to E) activity alone or in the presence of 1.91 µM of Pp*a* (IC_{50}) plus light, (**c**) the dose-dependent activity of Fraction E from Cc alone or with 1.91 µM Pp*a* (IC_{50} value) plus light. No treat means without Cc. Control cells were incubated with complete cell medium and DMSO. Results are expressed as percent survival after 24 h exposure followed by 1 h photo-activation (* $p < 0.05$; ** $p < 0.01$; *** $p < 0.001$).

3.3. Mechanism of Action at Gene and Protein Level

PCR array for A2058 cells treated in the presence of Pp*a* 1.91 µM or fraction E 10 µg·mL^{-1} or a combination of Pp*a* 1.91 µM and fraction E, each followed by 1 h photo-activation, showed a series of up- or down-regulated genes (Table 2). Some of these genes were common to the three treatments, while others were peculiar to a specific treatment (Table 2). For instance, the three treatments induced the up-regulation of tumor necrosis factor, estrogen receptor 1 and defensin beta 1, while they decreased the expression of amyloid beta (A4) precursor protein, "glucosidase, alpha; acid" and transmembrane protein 57. The combination treatment of fraction E with Pp*a* and photo-activation was the only treatment able to also induce the decreased expression of tumor necrosis factor receptor superfamily, member 1A, cathepsin S and cathepsin B (Table 2).

Table 2. Expression levels of cell death-related genes.

UniGEne	RefSeq	Symbol	Description	Fold	SD
Genes Up-Regulated by Pheophorbide *a* Treatment plus Photo-Activation					
Hs.632469	NM_020387	RAB25	RAB25, member RAS oncogene family	3.84	0.00082
Hs.241570	NM_000594	TNF	Tumor necrosis factor	3.06	0.00033
Hs.744830	NM_000125	ESR1	Estrogen receptor 1	2.44	0.00021
Hs.643440	NM_002361	MAG	Myelin associated glycoprotein	2.38	0.00017
Hs.32949	NM_005218	DEFB1	Defensin, beta 1	2.20	0.00019
Hs.2007	NM_000639	FASLG	Fas ligand (TNF superfamily, member 6)	2.02	0.00019
Genes down-regulated by Pheophorbide *a* treatment plus photo-activation					
Hs.434980	NM_000484	APP	Amyloid beta (A4) precursor protein	–3.48	0.10040
Hs.189782	NM_018202	TMEM57	Transmembrane protein 57	–2.80	0.00419
Hs.1437	NM_000152	GAA	Glucosidase, alpha; acid	–2.47	0.00531
Hs.269027	NM_014568	GALNT5	UDP-N-acetyl-alpha-D-galactosamine:polypeptide N-acetylgalactosaminyltransferase 5 (GalNAc-T5)	–2.41	0.00010
Hs.171844	NM_006505	PVR	Poliovirus receptor	–2.07	0.02680
Genes up-regulated by Fraction E plus photo-activation					
Hs.744830	NM_000125	ESR1	Estrogen receptor 1	5.59	0.00049
Hs.472860	NM_001250	CD40	CD40 molecule, TNF receptor superfamily member 5	4.17	0.00028
Hs.241570	NM_000594	TNF	Tumor necrosis factor	3.75	0.00040
Hs.592244	NM_000074	CD40LG	CD40 ligand	2.30	0.00019
Hs.32949	NM_005218	DEFB1	Defensin, beta 1	2.30	0.00020
Hs.87236	NM_012188	FOXI 1	Forkhead box I1	2.30	0.00019
Hs.856	NM_000619	IFNG	Interferon, gamma	2.30	0.00021
Hs.700350	NM_000207	INS	Insulin	2.30	0.00020
Hs.519680	NM_001145805	IRGM	Immunity-related GTPase family, M	2.30	0.00090
Hs.592068	NM_020655	JPH3	Junctophilin 3	2.30	0.00022
Hs.553833	NM_001004467	OR10J3	Olfactory receptor, family 10, subfamily J, member 3	2.30	0.00020
Hs.442337	NM_176823	S100A7A	S100 calcium-binding protein A7A	2.30	0.00020
Hs.632469	NM_020387	RAB25	RAB25, member RAS oncogene family	2.14	0.00046
Hs.2007	NM_000639	FASLG	Fas ligand (TNF superfamily, member 6)	2.09	0.00020
Genes down-regulated by Fraction E plus photo-activation					
Hs.591834	NM_003844	TNFRSF10A	Tumor necrosis factor receptor superfamily, member 10a	–4.35	0.00046
Hs.434980	NM_000484	APP	Amyloid beta (A4) precursor protein	–2.73	0.13269
Hs.1437	NM_000152	GAA	Glucosidase, alpha; acid	–2.59	0.00507
Hs.189782	NM_018202	TMEM57	Transmembrane protein 57	–2.19	0.00537
Hs.643120	NM_000875	IGF1R	Insulin-like growth factor 1 receptor	–2.15	0.02531
Genes up-regulated by Pheophorbide *a* and Fraction E treatment plus photo-activation					
Hs.241570	NM_000594	TNF	Tumor necrosis factor	3.75	0.00040
Hs.744830	NM_000125	ESR1	Estrogen receptor 1	3.67	0.00032
Hs.592068	NM_020655	JPH3	Junctophilin 3	2.55	0.00022
Hs.592244	NM_000074	CD40LG	CD40 ligand	2.19	0.00024
Hs.32949	NM_005218	DEFB1	Defensin, beta 1	2.19	0.00019
Hs.87236	NM_012188	FOXI 1	Forkhead box I1	2.19	0.00019
Hs.856	NM_000619	IFNG	Interferon, gamma	2.19	0.00132
Hs.700350	NM_000207	INS	Insulin	2.19	0.00019
Hs.519680	NM_001145805	IRGM	Immunity-related GTPase family, M	2.19	0.00021
Hs.553833	NM_001004467	OR10J3	Olfactory receptor, family 10, subfamily J, member 3	2.19	0.00009
Hs.442337	NM_176823	S100A7A	S100 calcium binding protein A7A	2.19	0.000019
Genes down-regulated by Pheophorbide *a* and Fraction E treatment plus photo-activation					
Hs.434980	NM_000484	APP	Amyloid beta (A4) precursor protein	–9.80	0.03694
Hs.1437	NM_000152	GAA	Glucosidase, alpha; acid	–4.91	0.00267
Hs.269027	NM_014568	GALNT5	UDP-N-acetyl-alpha-D-galactosamine:polypeptide N-acetylgalactosaminyltransferase 5 (GalNAc-T5)	–4.39	0.00055

Table 2. *Cont.*

UniGEne	RefSeq	Symbol	Description	Fold	SD
Hs.189782	NM_018202	TMEM57	Transmembrane protein 57	–4.24	0.00277
Hs.591834	NM_003844	TNFRSF10A	Tumor necrosis factor receptor superfamily, member 10a	–3.72	0.00042
Hs.171844	NM_006505	PVR	Poliovirus receptor	–3.70	0.01497
Hs.643120	NM_000875	IGFR1	Insulin-like growth factor 1 receptor	–2.58	0.02103
Hs.713833	NM_001065	TNFRSF1A	Tumor necrosis factor receptor superfamily, member 1A	–2.54	0.01441
Hs.181301	NM_004079	CTSS	Cathepsin S	–2.46	0.00208
Hs.520898	NM_001908	CTSB	Cathepsin B	–2.17	0.01346

B-cell lymphoma-2 (Bcl-2) and Bcl-2-associated X protein (Bax) expression were also evaluated to better understand the mechanism of action induced. These two proteins are involved in the early stage of apoptotic processes [38,39]. Considering that Pp*a* treatment was reported to be associated with lipid peroxidation [40], the level of glutathione peroxidase 4 (GPX4) and nuclear receptor coactivator 4 (NCOA4) was also analyzed at the protein level. GPX4 is known to protect membrane lipids against peroxidation; indeed, GPX4 reduction has been associated with lipid peroxide accumulation [41]. NCOA4 is responsible for ferritin transport to lysosomes and degradation [42], impairing iron trafficking [43]. Our results showed that Pp*a* treatment induced a significant reduction in Bcl-2, GPX4, and NCOA4 protein levels (Figures 2a–d and S2a), and it did not affect Bax protein levels (Figures 2a and S2b). *Cc* Fraction E treatment induced a reduction in Bcl-2 and NCOA4 (Figures 2a,b,d and S2a) and increased the level of Bax protein Figures 2a and S2b). Combination treatment by testing Pp*a*, Cc fraction E plus photo-activation reduced Bcl-2, GPX4, and NCOA4 protein levels (Figures 2a–d and S2a), and increased Bax protein level (Figures 2a,b and S2b). The reduction in the Bcl-2/Bax ratio triggered the mitochondrial-dependent apoptotic pathway [38,44]. Loss of NCOA4 led to ferritin accumulation [42] and tumor growth suppression in melanoma cell models [45]. β-tubulin, initially selected as a possible reference gene for Western blotting, was also found to be differentially expressed (Figure 2e).

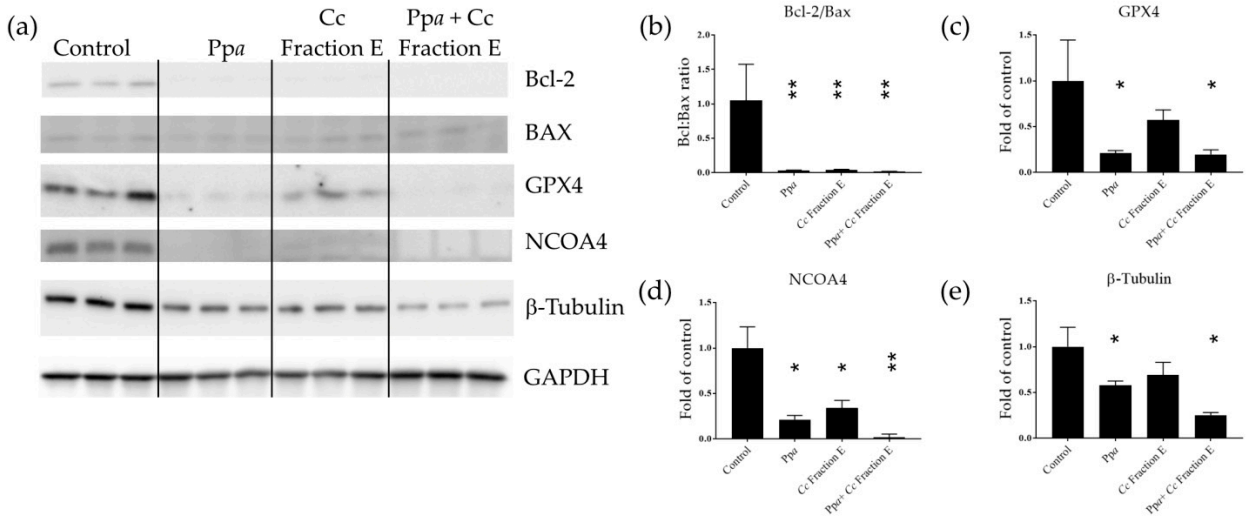

Figure 2. Western blotting analyses. (**a**) Immunodetection of Bcl-2, Bax, GPX4, NCOA4 and beta-tubulin in treated cells with Pp*a*, Cc fraction E or both, followed by photo-activation; (**b**) Bcl-2/Bax ratio; (**c**) band intensity for GPX4, (**d**) NCOA4, (**e**) β-Tubulin normalized with glyceraldehyde 3-phosphate dehydrogenase (GAPDH) (* $p < 0.05$; ** $p < 0.01$).

4. Discussion

Looking for new therapeutics and combinations of drugs leading to higher cancer selectivity and fewer side effects is still a big challenge. Pp*a* is a chlorophyll degradation product which has been shown to exert anticancer properties with or without photo-activation; the so-called photodynamic therapy [3]. Our data show that the most active combination against melanoma cells was induced by fraction E from the diatom *Cylindrotheca closterium*, plus Pp*a* followed by 1 h photo-activation. In a previous study, we showed the composition of *C. closterium* fractions A–D [31] and suggested that the anti-inflammatory activity observed for *C. closterium* fractions C and D was related to the presence of lysophosphatidylcholines and the chlorophyll-derived molecules Pp*a* and hydroxypheophorbide *a* [31]. Compared to fractions A–D, fractions E also contained a larger amount of Pheophytin *a*, which also is a breakdown product of chlorophyll but it has a long aliphatic tail making it more non-polar (unpublished data). This composition difference in the fractions may explain why fraction E is more active compared to the others. Pheophytin *a* isolated from the seagrass *Syringodium isoetifolium* also showed anticancer properties against adenocarcinomic A549 cells [46]. Similarly, Pheophytin *a* from the plant *Leucaena leucocephala* showed anticancer, anti-migration and anti-invasion activity in human gastric cancer cell line (AGS) [47].

When we studied the mechanism of action in the current study, Pp*a* triggered the mitochondrial-related apoptotic pathway in melanoma cells as also previously reported in hepatocellular carcinoma [4], uterine carcinosarcoma [5] and breast tumor [7]. Our results suggested the activation of the intrinsic apoptotic pathway (Bcl-2/Bax disregulation) triggered by Pp*a* and *Cc* fraction E treatment followed by 1 h photo-activation. Other transcripts have been found to be differentially expressed as well. Up-regulated genes by Pp*a*, fraction E or the combination of both plus photo-activation included TNF, estrogen receptor and defensin beta 1. The role of TNF in melanoma is still controversial [48]. TNF has been shown to have a key role in immunity and immunomodulation and is associated with both the inhibition and promotion of tumor proliferation [48,49]. The role of the estrogen receptor in melanoma progression and genesis is still under investigation [50]. Hoi et al. [7] also showed that Pp*a* does not require the estrogen receptor for transport into cells. Defensin beta 1 has been found to be constitutively expressed in various epithelia [51,52]. Moreover, defensin beta 1 was reduced in squamous cell carcinoma and its down-regulation was directly related to malignancy transformation [53]. Defensin beta 1 was also down-regulated in prostate carcinomas [54] and in renal cell carcinomas (RCC) [55]. The down-regulated transcripts by the three treatments also included the amyloid beta precursor, a glucosidase alpha acid and a transmembrane protein 57. The amyloid beta precursor protein has been always linked to Alzheimer disease, but recently, the increased expression of this protein has been found in multiple types of cancers [56]. Hence, its down-regulation is in line with the reduction in cancer cell proliferation. A transcript coding for "glucosidase, alpha; acid", also known as acid alpha-glucosidase (GAA), is a lysosomal enzyme, and its suppression has shown to be associated with improved chemosensitivity and apoptosis in pancreatic cancer cells [57]. Hamura et al. [57] found a reduction in tumor growth and prolonged tumor-related survival after GAA silencing in a murine model. In addition, apoptosis activation was also observed. Transmembrane proteins have been found to be differentially expressed in different tumors, but their function is still mostly unknown [58]. Finally, treatment with Pp*a* plus fraction E plus photo-activation also induced the down-regulation of tumor necrosis factor receptor superfamily (member 1A), cathepsin B and S. Tumor necrosis receptor 1 levels were found to be increased in patients with hepatocellular carcinoma [49], but to our knowledge its dysregulation has never been reported to be associated with melanoma. Cathepsin B inhibition has been found to reduce cell invasiveness of melanoma cells [59]. Cathepsin S has been associated with different cancer types. It is a mediator of tumor progression and has been associated with angiogenesis and metastasis formation, hence, representing a promising target for cancer therapy [60].

The microtubule subunit β-tubulin, initially selected as a possible reference gene for Western blotting, was also found to be differentially expressed (i.e., reduced expression induced by the treatment) in our study. In fact, levels of β-tubulin were affected by Pp*a* treatment. The intrinsic apoptotic pathway has been found to also be activated by chemotherapeutic agents targeting tubulin proteins, such as paclitaxel (Taxol®) and docetaxel [61]. However, in addition to the intrinsic apoptotic pathway mediators, we also found that GPX4 and NCOA4 protein levels were reduced after Pp*a* treatment and photo-activation suggesting that the treatment may induce lipid peroxidation.

This study shows that the known compound Pp*a*, a specific microalgal fraction plus photo-activation, can have an additive anti-proliferative role on melanoma cells. As reported by Prüser et al. [62], the US Food and Drug Administration (FDA) has granted the GRAS status to various microalgae, including *Auxenochlorella protothecoides* (formerly *Chlorella protothecoides*), *Spirulina*, *Dunaliella salina*, *Haematococcus pluvialis*, *Prototheca zopfii*, *Ulkenia* sp., *Crypthecodinium cohnii* and *Schizochytrium* sp. For some of these, the GRAS status refers to the entire biomass, while for others only a part of the extract or a fraction. *Spirulina* and *Chlorella* are most commonly used in Europe and, recently, whole alga (*Odontella aurita* and *Tetraselmis chui*) or only specific components (*Ulkenia* sp. oil, *Schizochytrium* sp. oil, *Haematococcus pluvialis* oleoresin) have been approved under the Commission Implementing Regulation (EU) 2017/2470 [62]. This "safe" status has been expanded to a greater number of species in recent years and this trend will positively influence the addition of microalgal extracts, fractions and components in nutraceutical and pharmaceutical products. These may have properties that are useful for various human pathologies, such as antioxidant, anti-inflammatory and anticancer properties [12,31]. Future studies on the combinatorial effects of microalgal extracts with known drugs, such as those used for chemotherapy, with or without photo-activation, can shed light on new activities against cancer cells and on possible photodynamic therapies.

Supplementary Materials: The following supporting information can be downloaded at: https://www.mdpi.com/article/10.3390/app13042590/s1, Figure S1: Antiproliferative activity of the diatom *Cylindrotheca closterium*, Pheophorbide *a*, and their combination on normal human cells HACAT. Results are expressed as percent survival after 24 h exposure followed by 1 h photo-activation (* $p < 0.05$; ** $p < 0.01$; *** $p < 0.001$); Figure S2: The intensity of the bands of immunodetected Bcl-2 (a) and Bax (b) were normalized with glyceraldehyde 3-phosphate dehydrogenase (GAPDH) (* $p < 0.05$; ** $p < 0.01$); Table S1: Antiproliferative activity of various microalgae on cancer human cells.

Author Contributions: Conceptualization, A.S., A.I. and C.L.; formal analysis, A.S., G.R. and C.L.; writing—original draft preparation, A.S., G.R. and C.L.; writing—review and editing, A.S., G.R., A.I. and C.L.; supervision, A.I. and C.L. All authors have read and agreed to the published version of the manuscript.

Funding: This research was supported by the project "Antitumor Drugs and Vaccines from the Sea (ADViSE)" (CUP B43D18000240007–SURF 17061BP000000011; PG/2018/0494374) funded by POR Campania FESR 2014–2020 "Technology Platform for Therapeutic Strategies against Cancer"-Action 1.1.2 and 1.2.2. Assunta Saide and Gennaro Riccio were supported by research grants within this project.

Institutional Review Board Statement: Not applicable.

Informed Consent Statement: Not applicable.

Data Availability Statement: Not applicable.

Acknowledgments: Authors thank the Servier Medical Art (SMART) website (https://smart.servier.com/; accessed on 1 February 2022) by Servier for elements in the graphical abstract and PubChem (https://pubchem.ncbi.nlm.nih.gov/compound/Pheophorbide-a#section=3D-Conformer; accessed on 18 April 2022) for the 3D structure of Pheophorbide *a*. Authors thank Massimo Perna and Mariano Amoroso for their technical support. Authors also thanks Espen H. Hansen from The Arctic University of Norway (UiT), Norway, for dereplication support.

Conflicts of Interest: The authors declare no conflict of interest.

References

1. Dobson, J.; de Queiroz, G.F.; Golding, J.P. Photodynamic Therapy and Diagnosis: Principles and Comparative Aspects. *Vet. J.* **2018**, *233*, 8–18. [CrossRef] [PubMed]
2. Wachowska, M.; Muchowicz, A.; Firczuk, M.; Gabrysiak, M.; Winiarska, M.; Wańczyk, M.; Bojarczuk, K.; Golab, J. Aminolevulinic Acid (ALA) as a Prodrug in Photodynamic Therapy of Cancer. *Molecules* **2011**, *16*, 4140–4164. [CrossRef]
3. Saide, A.; Lauritano, C.; Ianora, A. Pheophorbide *a*: State of the Art. *Mar. Drugs* **2020**, *18*, 257. [CrossRef] [PubMed]
4. Tang, P.M.-K.; Chan, J.Y.-W.; Au, S.W.-N.; Kong, S.-K.; Tsui, S.K.-W.; Waye, M.M.-Y.; Mak, T.C.-W.; Fong, W.-P.; Fung, K.-P. Pheophorbide *a*, an Active Compound Isolated from Scutellaria Barbata, Possesses Photodynamic Activities by Inducing Apoptosis in Human Hepatocellular Carcinoma. *Cancer Biol. Ther.* **2006**, *5*, 1111–1116. [CrossRef] [PubMed]
5. Tang, P.M.-K.; Liu, X.-Z.; Zhang, D.-M.; Fong, W.-P.; Fung, K.-P. Pheophorbide *a* Based Photodynamic Therapy Induces Apoptosis via Mitochondrial-Mediated Pathway in Human Uterine Carcinosarcoma. *Cancer Biol. Ther.* **2009**, *8*, 533–539. [CrossRef]
6. Bui-Xuan, N.-H.; Tang, P.M.-K.; Wong, C.-K.; Fung, K.-P. Photo-Activated Pheophorbide-a, an Active Component of Scutellaria Barbata, Enhances Apoptosis via the Suppression of ERK-Mediated Autophagy in the Estrogen Receptor-Negative Human Breast Adenocarcinoma Cells MDA-MB-231. *J. Ethnopharmacol.* **2010**, *131*, 95–103. [CrossRef]
7. Hoi, S.W.-H.; Wong, H.M.; Chan, J.Y.-W.; Yue, G.G.L.; Tse, G.M.-K.; Law, B.K.-B.; Fong, W.P.; Fung, K.P. Photodynamic Therapy of Pheophorbide *a* Inhibits the Proliferation of Human Breast Tumour via Both Caspase-Dependent and -Independent Apoptotic Pathways in In Vitro and In Vivo Models. *Phytother. Res.* **2012**, *26*, 734–742. [CrossRef]
8. Ahn, M.Y.; Yoon, H.-E.; Kwon, S.-M.; Lee, J.; Min, S.-K.; Kim, Y.-C.; Ahn, S.-G.; Yoon, J.-H. Synthesized Pheophorbide A-Mediated Photodynamic Therapy Induced Apoptosis and Autophagy in Human Oral Squamous Carcinoma Cells. *J. Oral Pathol. Med.* **2013**, *42*, 17–25. [CrossRef]
9. Cho, M.; Park, G.-M.; Kim, S.-N.; Amna, T.; Lee, S.; Shin, W.-S. Glioblastoma-Specific Anticancer Activity of Pheophorbide *a* from the Edible Red Seaweed Grateloupia Elliptica. *J. Microbiol. Biotechnol.* **2014**, *24*, 346–353. [CrossRef]
10. Lauritano, C.; Andersen, J.H.; Hansen, E.; Albrigtsen, M.; Escalera, L.; Esposito, F.; Helland, K.; Hanssen, K.Ø.; Romano, G.; Ianora, A. Bioactivity Screening of Microalgae for Antioxidant, Anti-Inflammatory, Anticancer, Anti-Diabetes, and Antibacterial Activities. *Front. Mar. Sci.* **2016**, *3*, 68. [CrossRef]
11. Romano, G.; Costantini, M.; Sansone, C.; Lauritano, C.; Ruocco, N.; Ianora, A. Marine Microorganisms as a Promising and Sustainable Source of Bioactive Molecules. *Mar. Environ. Res.* **2017**, *128*, 58–69. [CrossRef] [PubMed]
12. Saide, A.; Martínez, K.A.; Ianora, A.; Lauritano, C. Unlocking the Health Potential of Microalgae as Sustainable Sources of Bioactive Compounds. *Int. J. Mol. Sci.* **2021**, *22*, 4383. [CrossRef] [PubMed]
13. Lauritano, C.; Ianora, A. Marine Organisms with Anti-Diabetes Properties. *Mar. Drugs* **2016**, *14*, 220. [CrossRef] [PubMed]
14. Martínez Andrade, K.; Lauritano, C.; Romano, G.; Ianora, A. Marine Microalgae with Anti-Cancer Properties. *Mar. Drugs* **2018**, *16*, 165. [CrossRef]
15. Martínez, K.A.; Lauritano, C.; Druka, D.; Romano, G.; Grohmann, T.; Jaspars, M.; Martín, J.; Díaz, C.; Cautain, B.; de la Cruz, M.; et al. Amphidinol 22, a New Cytotoxic and Antifungal Amphidinol from the Dinoflagellate *Amphidinium Carterae*. *Mar. Drugs* **2019**, *17*, 385. [CrossRef]
16. Martínez, K.A.; Saide, A.; Crespo, G.; Martín, J.; Romano, G.; Reyes, F.; Lauritano, C.; Ianora, A. Promising Antiproliferative Compound From the Green Microalga Dunaliella Tertiolecta Against Human Cancer Cells. *Front. Mar. Sci.* **2022**, *9*, 778108. [CrossRef]
17. Riccio, G.; Lauritano, C. Microalgae with Immunomodulatory Activities. *Mar. Drugs* **2020**, *18*, 2. [CrossRef]
18. Giordano, D.; Costantini, M.; Coppola, D.; Lauritano, C.; Núñez Pons, L.; Ruocco, N.; di Prisco, G.; Ianora, A.; Verde, C. Biotechnological Applications of Bioactive Peptides From Marine Sources. In *Advances in Microbial Physiology*; Elsevier: Amsterdam, The Netherlands, 2018; Volume 73, pp. 171–220. ISBN 978-0-12-815190-7.
19. Brillatz, T.; Lauritano, C.; Jacmin, M.; Khamma, S.; Marcourt, L.; Righi, D.; Romano, G.; Esposito, F.; Ianora, A.; Queiroz, E.F.; et al. Zebrafish-Based Identification of the Antiseizure Nucleoside Inosine from the Marine Diatom Skeletonema Marinoi. *PLoS ONE* **2018**, *13*, e0196195. [CrossRef]
20. Lauritano, C.; Martín, J.; de la Cruz, M.; Reyes, F.; Romano, G.; Ianora, A. First Identification of Marine Diatoms with Anti-Tuberculosis Activity. *Sci. Rep.* **2018**, *8*, 2284. [CrossRef]
21. Riccio, G.; Ruocco, N.; Mutalipassi, M.; Costantini, M.; Zupo, V.; Coppola, D.; de Pascale, D.; Lauritano, C. Ten-Year Research Update Review: Antiviral Activities from Marine Organisms. *Biomolecules* **2020**, *10*, 1007. [CrossRef]
22. Muller-Feuga, A. The Role of Microalgae in Aquaculture: Situation and Trends. *J. Appl. Phycol.* **2000**, *12*, 527–534. [CrossRef]
23. Hossain, N.; Mahlia, T.M.I.; Saidur, R. Latest Development in Microalgae-Biofuel Production with Nano-Additives. *Biotechnol. Biofuels* **2019**, *12*, 125. [CrossRef] [PubMed]
24. Orejuela-Escobar, L.; Gualle, A.; Ochoa-Herrera, V.; Philippidis, G.P. Prospects of Microalgae for Biomaterial Production and Environmental Applications at Biorefineries. *Sustainability* **2021**, *13*, 3063. [CrossRef]
25. Pulz, O.; Gross, W. Valuable Products from Biotechnology of Microalgae. *Appl. Microbiol. Biotechnol.* **2004**, *65*, 635–648. [CrossRef] [PubMed]
26. Eryalçın, K.M. Nutritional Value and Production Performance of the Rotifer Brachionus Plicatilis Müller, 1786 Cultured with Different Feeds at Commercial Scale. *Aquac. Int.* **2019**, *27*, 875–890. [CrossRef]
27. Torres-Tiji, Y.; Fields, F.J.; Mayfield, S.P. Microalgae as a Future Food Source. *Biotechnol. Adv.* **2020**, *41*, 107536. [CrossRef]

28. Gouveia, L.; Coutinho, C.; Mendonça, E.; Batista, A.P.; Sousa, I.; Bandarra, N.M.; Raymundo, A. Functional Biscuits with PUFA-Ω3 from Isochrysis Galbana. *J. Sci. Food Agric.* **2008**, *88*, 891–896. [CrossRef]
29. Fradique, M.; Batista, A.P.; Nunes, C.M.; Gouveia, L.; Bandarra, N.M.; Raymundo, A. Isochrysis Galbana and Diacronema Vlkianum Biomass Incorporation in Pasta Products as PUFA's Source. *LWT—Food Sci. Technol.* **2013**, *50*, 312–319. [CrossRef]
30. Matos, J.; Afonso, C.; Cardoso, C.; Serralheiro, M.L.; Bandarra, N.M. Yogurt Enriched with Isochrysis Galbana: An Innovative Functional Food. *Foods* **2021**, *10*, 1458. [CrossRef]
31. Lauritano, C.; Helland, K.; Riccio, G.; Andersen, J.H.; Ianora, A.; Hansen, E. Lysophosphatidylcholines and Chlorophyll-Derived Molecules from the Diatom Cylindrotheca Closterium with Anti-Inflammatory Activity. *Mar. Drugs* **2020**, *18*, 166. [CrossRef]
32. Pasquet, V.; Morisset, P.; Ihammouine, S.; Chepied, A.; Aumailley, L.; Berard, J.-B.; Serive, B.; Kaas, R.; Lanneluc, I.; Thiery, V.; et al. Antiproliferative Activity of Violaxanthin Isolated from Bioguided Fractionation of Dunaliella Tertiolecta Extracts. *Mar. Drugs* **2011**, *9*, 819–831. [CrossRef] [PubMed]
33. Guillard, R.R.L. Culture of Phytoplankton for Feeding Marine Invertebrates. In *Culture of Marine Invertebrate Animals: Proceedings—1st Conference on Culture of Marine Invertebrate Animals Greenport*; Smith, W.L., Chanley, M.H., Eds.; Springer: Boston, MA, USA, 1975; pp. 29–60. ISBN 978-1-4615-8714-9.
34. Keller, M.D.; Selvin, R.C.; Claus, W.; Guillard, R.R.L. Media for the Culture of Oceanic Ultraphytoplankton1,2. *J. Phycol.* **1987**, *23*, 633–638. [CrossRef]
35. Ribalet, F.; Wichard, T.; Pohnert, G.; Ianora, A.; Miralto, A.; Casotti, R. Age and Nutrient Limitation Enhance Polyunsaturated Aldehyde Production in Marine Diatoms. *Phytochemistry* **2007**, *9*, 2059–2067. [CrossRef] [PubMed]
36. Cutignano, A.; Nuzzo, G.; Ianora, A.; Luongo, E.; Romano, G.; Gallo, C.; Sansone, C.; Aprea, S.; Mancini, F.; D'Oro, U.; et al. Development and Application of a Novel SPE-Method for Bioassay-Guided Fractionation of Marine Extracts. *Mar. Drugs* **2015**, *13*, 5736–5749. [CrossRef]
37. Riccio, G.; Nuzzo, G.; Zazo, G.; Coppola, D.; Senese, G.; Romano, L.; Costantini, M.; Ruocco, N.; Bertolino, M.; Fontana, A.; et al. Bioactivity Screening of Antarctic Sponges Reveals Anticancer Activity and Potential Cell Death via Ferroptosis by Mycalols. *Mar. Drugs* **2021**, *19*, 459. [CrossRef]
38. Singh, R.; Letai, A.; Sarosiek, K. Regulation of Apoptosis in Health and Disease: The Balancing Act of BCL-2 Family Proteins. *Nat. Rev. Mol. Cell Biol.* **2019**, *20*, 175–193. [CrossRef]
39. Korsmeyer, S.J.; Shutter, J.R.; Veis, D.J.; Merry, D.E.; Oltvai, Z.N. Bcl-2/Bax: A Rheostat That Regulates an Anti-Oxidant Pathway and Cell Death. *Semin. Cancer Biol.* **1993**, *4*, 327–332.
40. Rapozzi, V.; Miculan, M.; Xodo, L. Evidence That Photoactivated Pheophorbide *a* Causes in Human Cancer Cells a Photodynamic Effect Involving Lipid Peroxidation. *Cancer Biol. Ther.* **2009**, *8*, 1318–1327. [CrossRef]
41. Li, J.; Cao, F.; Yin, H.; Huang, Z.; Lin, Z.; Mao, N.; Sun, B.; Wang, G. Ferroptosis: Past, Present and Future. *Cell Death Dis.* **2020**, *11*, 88. [CrossRef]
42. Santana-Codina, N.; Mancias, J.D. The Role of NCOA4-Mediated Ferritinophagy in Health and Disease. *Pharmaceuticals* **2018**, *11*, 114. [CrossRef]
43. Ryu, M.-S.; Zhang, D.; Protchenko, O.; Shakoury-Elizeh, M.; Philpott, C.C. PCBP1 and NCOA4 Regulate Erythroid Iron Storage and Heme Biosynthesis. *J. Clin. Investig.* **2017**, *127*, 1786–1797. [CrossRef] [PubMed]
44. Raisova, M.; Hossini, A.M.; Eberle, J.; Riebeling, C.; Wieder, T.; Sturm, I.; Daniel, P.T.; Orfanos, C.E.; Geilen, C.C. The Bax/Bcl-2 Ratio Determines the Susceptibility of Human Melanoma Cells to CD95/Fas-Mediated Apoptosis. *J. Investig. Dermatol.* **2001**, *117*, 333–340. [CrossRef] [PubMed]
45. Shekoohi, S.; Rajasekaran, S.; Patel, D.; Yang, S.; Liu, W.; Huang, S.; Yu, X.; Witt, S.N. Knocking out Alpha-Synuclein in Melanoma Cells Dysregulates Cellular Iron Metabolism and Suppresses Tumor Growth. *Sci. Rep.* **2021**, *11*, 5267. [CrossRef] [PubMed]
46. Shailaja, V.L.; Christina, V.S.; Mohanapriya, C.D.; Sneha, P.; Lakshmi Sundaram, R.; Magesh, R.; George Priya Doss, C.; Gnanambal, K.M.E. A Natural Anticancer Pigment, Pheophytin a, from a Seagrass Acts as a High Affinity Human Mitochondrial Translocator Protein (TSPO) Ligand, in Silico, to Reduce Mitochondrial Membrane Potential (Δψmit) in Adenocarcinomic A549 Cells. *Phytomedicine* **2019**, *61*, 152858. [CrossRef]
47. Chen, C.-Y. The Anti-Cancer and Anti-Metastasis Effects of Phytochemical Constituents from Leucaena Leucocephala. *Biomed. Res.* **2017**, *28*, 2893–2897.
48. Donia, M.; Kjeldsen, J.W.; Svane, I.M. The Controversial Role of TNF in Melanoma. *OncoImmunology* **2016**, *5*, e1107699. [CrossRef]
49. Puimège, L.; Libert, C.; Van Hauwermeiren, F. Regulation and Dysregulation of Tumor Necrosis Factor Receptor-1. *Cytokine Growth Factor Rev.* **2014**, *25*, 285–300. [CrossRef]
50. Dika, E.; Patrizi, A.; Lambertini, M.; Manuelpillai, N.; Fiorentino, M.; Altimari, A.; Ferracin, M.; Lauriola, M.; Fabbri, E.; Campione, E.; et al. Estrogen Receptors and Melanoma: A Review. *Cells* **2019**, *8*, 1463. [CrossRef]
51. Weinberg, A.; Jin, G.; Sieg, S.; McCormick, T. The Yin and Yang of Human Beta-Defensins in Health and Disease. *Front. Immunol.* **2012**, *3*, 294. [CrossRef]
52. O'Neil, D.A.; Porter, E.M.; Elewaut, D.; Anderson, G.M.; Eckmann, L.; Ganz, T.; Kagnoff, M.F. Expression and Regulation of the Human β-Defensins HBD-1 and HBD-2 in Intestinal Epithelium. *J. Immunol.* **1999**, *163*, 6718–6724. [CrossRef]
53. Scola, N.; Gambichler, T.; Saklaoui, H.; Bechara, F.G.; Georgas, D.; Stücker, M.; Gläser, R.; Kreuter, A. The Expression of Antimicrobial Peptides Is Significantly Altered in Cutaneous Squamous Cell Carcinoma and Precursor Lesions. *Br. J. Dermatol.* **2012**, *167*, 591–597. [CrossRef] [PubMed]

54. Donald, C.D.; Sun, C.Q.; Lim, S.D.; Macoska, J.; Cohen, C.; Amin, M.B.; Young, A.N.; Ganz, T.A.; Marshall, F.F.; Petros, J.A. Cancer-Specific Loss of β-Defensin 1 in Renal and Prostatic Carcinomas. *Lab. Investig.* **2003**, *83*, 501–505. [CrossRef] [PubMed]
55. Young, A.N.; Amin, M.B.; Moreno, C.S.; Lim, S.D.; Cohen, C.; Petros, J.A.; Marshall, F.F.; Neish, A.S. Expression Profiling of Renal Epithelial Neoplasms: A Method for Tumor Classification and Discovery of Diagnostic Molecular Markers. *Am. J. Pathol.* **2001**, *158*, 1639–1651. [CrossRef] [PubMed]
56. Lim, S.; Yoo, B.K.; Kim, H.-S.; Gilmore, H.L.; Lee, Y.; Lee, H.; Kim, S.-J.; Letterio, J.; Lee, H. Amyloid-β Precursor Protein Promotes Cell Proliferation and Motility of Advanced Breast Cancer. *BMC Cancer* **2014**, *14*, 928. [CrossRef] [PubMed]
57. Hamura, R.; Shirai, Y.; Shimada, Y.; Saito, N.; Taniai, T.; Horiuchi, T.; Takada, N.; Kanegae, Y.; Ikegami, T.; Ohashi, T.; et al. Suppression of Lysosomal Acid Alpha-Glucosidase Impacts the Modulation of Transcription Factor EB Translocation in Pancreatic Cancer. *Cancer Sci.* **2021**, *112*, 2335–2348. [CrossRef] [PubMed]
58. Schmit, K.; Michiels, C. TMEM Proteins in Cancer: A Review. *Front. Pharmacol.* **2018**, *9*, 1345. [CrossRef]
59. Matarrese, P.; Ascione, B.; Ciarlo, L.; Vona, R.; Leonetti, C.; Scarsella, M.; Mileo, A.M.; Catricalà, C.; Paggi, M.G.; Malorni, W. Cathepsin B Inhibition Interferes with Metastatic Potential of Human Melanoma: An in Vitro and in Vivo Study. *Mol. Cancer* **2010**, *9*, 207. [CrossRef]
60. McDowell, S.H.; Gallaher, S.A.; Burden, R.E.; Scott, C.J. Leading the Invasion: The Role of Cathepsin S in the Tumour Microenvironment. *Biochim. Biophys. Acta BBA-Mol. Cell Res.* **2020**, *1867*, 118781. [CrossRef]
61. McGrogan, B.T.; Gilmartin, B.; Carney, D.N.; McCann, A. Taxanes, Microtubules and Chemoresistant Breast Cancer. *Biochim. Biophys. Acta BBA-Rev. Cancer* **2008**, *1785*, 96–132. [CrossRef]
62. Prüser, T.F.; Braun, P.G.; Wiacek, C. Microalgae as a Novel Food. *Ernahrungs Umsch.* **2021**, *68*, 78–85. [CrossRef]